PCP
PLANT & CELL PHYSIOLOGY

Inhibition of Recombinant Aldose-6-Phosphate Reductase from Peach Leaves by Hexose-Phosphates, Inorganic Phosphate and Oxidants

Matías D. Hartman[1,2], Carlos M. Figueroa[1,2], Diego G. Arias[1] and Alberto A. Iglesias[1,*]

[1]Instituto de Agrobiotecnología del Litoral, UNL, CONICET, FBCB, Colectora Ruta Nacional 168 km 0, 3000 Santa Fe, Argentina
[2]These authors contributed equally to this work.
*Corresponding author: E-mail, iglesias@fbcb.unl.edu.ar; Fax, +54-342-451-1370.
(Received August 22, 2016; Accepted October 17, 2016)

Regular Paper

Glucitol, also known as sorbitol, is a major photosynthetic product in plants from the Rosaceae family. This sugar alcohol is synthesized from glucose-6-phosphate by the combined activities of aldose-6-phosphate reductase (Ald6PRase) and glucitol-6-phosphatase. In this work we show the purification and characterization of recombinant Ald6PRase from peach leaves. The recombinant enzyme was inhibited by glucose-1-phosphate, fructose-6-phosphate, fructose-1,6-bisphosphate and orthophosphate. Oxidizing agents irreversibly inhibited the enzyme and produced protein precipitation. Enzyme thiolation with oxidized glutathione protected the enzyme from insolubilization caused by diamide, while incubation with $NADP^+$ (one of the substrates) completely prevented enzyme precipitation. Our results suggest that Ald6PRase is finely regulated to control carbon partitioning in peach leaves.

Keywords: Carbon partitioning • Glucitol • Peach • *Prunus persica* • Redox regulation • Sorbitol.

Abbreviations: AKRase, aldo-keto reductase; Ald6PRase, aldose-6-phosphate reductase; Di-E-GSSG, di-eosin-glutathione disulfide; DTT, dithiothreitol; Fru-1,6-bisP, fructose-1,6-bisphosphate; Fru-6P, fructose-6-phosphate; Ga3PDHase, glyceraldehyde-3-phosphate dehydrogenase; Glc-1P, glucose-1-phosphate; Glc-6P, glucose-6-phosphate; Gol, glucitol; Gol-6P, glucitol-6-phosphate; GolDHase, glucitol dehydrogenase; HEDS, 2-hydroxyethyl disulfide; Man-6P, mannose-6-phosphate; Man6PRase, mannose-6-phosphate reductase; 2ME, 2-mercaptoethanol; np, non-phosphorylating; *Ppe*, *Prunus persica*; TRX, thioredoxin.

Introduction

Plant carbon metabolism is finely orchestrated in order to provide carbon skeletons to the various metabolic pathways occurring in different intracellular compartments. Photosynthetic carbon fixation generates triose-phosphates, which are either used for starch synthesis within the chloroplast or exported to the cytosol for sucrose synthesis (Stitt et al. 2010, Figueroa et al. 2016). Intracellular carbon partitioning plays a key role for the production of the main photosynthates occurring in most plants, sucrose and starch. This process is crucial for both productivity and growth; consequently, the molecular mechanisms regulating sucrose and starch metabolism have been studied in detail (Ballicora et al. 2004, Stitt et al. 2010, MacRae and Lunn 2012, Figueroa et al. 2016). Sucrose is translocated from photosynthetic (source) to non-photosynthetic (sink) tissues, a process known as intercellular carbon partitioning. Once loaded into sink tissues, sucrose is cleaved by different enzymes and the products are directed to the hexose-P pool, which serves as a carbon source for multiple pathways (Stitt et al. 2010, Figueroa et al. 2016).

Some higher plants synthesize a sugar alcohol (in addition to sucrose and starch) as a major photosynthetic product. Nearly 20 sugar alcohols have been found in vascular plants, with 13 occurring in angiosperms (Moing 2000). Many economically important species (e.g. celery, coffee and olive) produce mannitol, while plants from the Rosaceae family (including apple, peach, plum, pear and apricot) synthesize glucitol (Gol) (Loescher and Everard 2004). Gol is not only a main photosynthetic product but also plays a role against abiotic stress. Like other compatible solutes, Gol levels rise in plants exposed to cold (Williams and Raese 1974, Hirai 1983), drought (Ranney et al. 1991) and salinity (Pommerrenig et al. 2007). Compatible solutes are accumulated in plants facing osmotic stress to repair the cytosolic imbalance (Hsiao et al. 1976). Osmolytes also scavenge reactive oxygen species and stabilize proteins and cell membranes from the damaging effects of desiccation (Hayat et al. 2012).

Gol is produced in the cytosol of source tissues from glucose-6-phosphate (Glc-6P) by the combined action of NADPH-dependent aldose-6-phosphate reductase (Ald6PRase; EC 1.1.1.200) and a specific Gol-6P phosphatase (EC 3.1.1.50). Gol is exported to heterotrophic or developing tissues, where it is converted into fructose (Fru) by an NAD^+-dependent Gol dehydrogenase (GolDHase; EC 1.1.1.14) (Loescher and Everard 2004, Figueroa et al. 2016). The synthesis of sugar alcohols requires reducing power (NADPH) to convert a hexose-P into a polyol-P, which could be supplied by the non-phosphorylating glyceraldehyde-3-phosphate dehydrogenase (np-Ga3PDHase;

Plant Cell Physiol. 58(1): 145–155 (2017) doi:10.1093/pcp/pcw180, Advance Access publication on 15 November 2016, available online at www.pcp.oxfordjournals.org

EC 1.2.1.9) (Rumpho et al. 1983, Gao and Loescher 2000). The synthesis and degradation of both sucrose and Gol are cytosolic (Loescher et al. 1982); thus, plant cells must finely regulate the enzymes involved in these routes to control carbon partitioning adequately.

Transcriptional control of Ald6PRase expression plays a key role in the source to sink transition in leaves from rosaceous species. The seminal work of Loescher et al. (1982) on apple trees showed that both the activity of Ald6PRase and Gol levels increase with leaf development during early spring. Similar seasonal changes in Ald6PRase activity were observed in loquat leaves (Hirai 1983). Later, Sakanishi et al. (1998) showed that Ald6PRase transcripts, protein and activity increase with leaf age. More recently, Li et al. (2007) reported that diurnal fluctuations of Gol levels in peach leaves are well correlated with Ald6PRase activity, suggesting that other mechanisms could be involved on the regulation of this enzyme.

There are several reports on Gol metabolism within plants from the Rosaceae family but only a few focusing on the enzymes involved in its metabolism (Negm and Loescher 1979, Hirai 1981, Negm and Loescher 1981, Kanayama and Yamaki 1993, Yamaguchi et al. 1994, Zhou et al. 2003a, Zhou et al. 2003b, Figueroa and Iglesias 2010), and even less dealing with their regulatory properties. We have recently reported the redox regulation of GolDHase from peach fruits by the homologous cytosolic thioredoxin (TRX) *h* (Hartman et al. 2014), constituting a spotlight regarding post-translational regulation of enzymes from Gol metabolism. In this scenario, developing tools for obtaining highly pure enzymes becomes essential. In this work we show the recombinant expression of Ald6PRase from peach leaves (*Ppe*Ald6PRase), its fine regulation by metabolites and post-translational modifications, and discuss their significance for the modulation of carbon partitioning in photosynthetic cells.

Results

Ald6PRase belongs to group 2 of the aldo-keto reductase (AKRase) superfamily (Hyndman et al. 2003). To deepen our knowledge of this group, we reconstructed a phylogenetic tree using sequences coding for *Ppe*Ald6PRase and homologous proteins from rosaceous plants and other species (**Fig. 1**; **Supplementary Dataset S1**). The resulting tree shows two major branches: one composed by 10 sequences from rosaceous plants (peach, apple, plum and pear) and another one containing sequences from a wide range of plant species, from the lycophyte *Selaginella moellendorffii* to eudicots (**Fig. 1**). Within the major branch, sequences from plants sharing certain features were clustered together, such as grasses and those from the Brassicaceae family (**Fig. 1**). Interestingly, three sequences from rosaceous plants were clustered in the major branch, clearly separated from other sequences from species of the Rosaceae family (**Fig. 1**, asterisk). Mannose-6P (Man-6P) reductase (Man6PRase; EC 1.1.1.224) from celery, which catalyzes the conversion of Man-6P into mannitol-1P, was clearly separated from all other sequences of the major branch (**Fig. 1**, star).

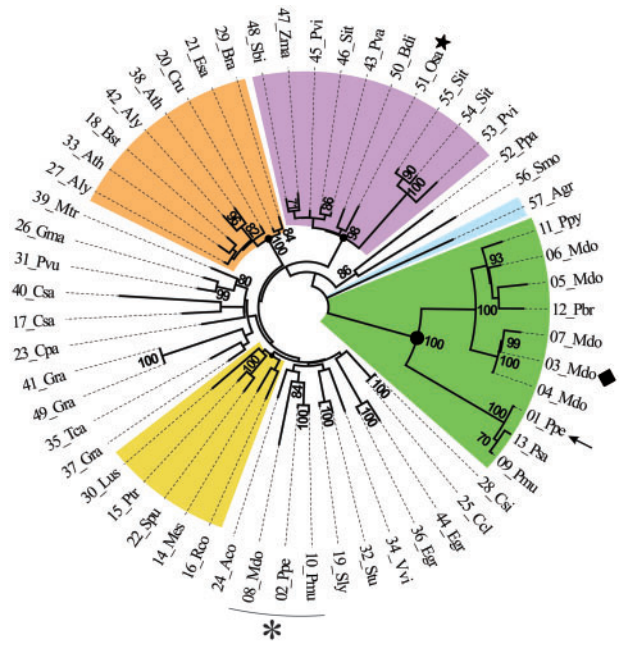

Fig. 1 Molecular phylogenetic analysis of plant AKRases. The tree was built using the maximum likelihood method, as described in the Materials and Methods. Two major branches can be observed: one including exclusively sequences from rosaceous plants (green shaded) and a second one containing sequences from multiple species. Branches starting with a circle correspond to clades with sequences from a particular group of plants: grasses (violet), Brassicaceae (orange) and Malphigiales (yellow). The black arrow points to peach Ald6PRase, which was used as query to find homologous AKRases; the star indicates celery Man6PRase; the diamond highlights apple Ald6PRase; the triangle shows rice Ald6PRase; and the asterisk denotes a group of protein sequences from rosaceous plants that are separated from the green shaded clade. Bootstrap values < 70 are not shown.

When we started this work, the peach genome project was at an early stage and there were no complete sequences for Ald6PRase. Nevertheless, we were able to clone a full open reading frame of 933 bp coding for a putative Ald6PRase using RNA from peach leaves, and the sequence was sent to the NCBI database (accession No. EF576940.2; **Fig. 1**, black arrow). This sequence is identical to that published after the peach genome was released (NCBI accession No. XP_007200459.1). The amplified cDNA encodes a putative protein of 310 amino acids with a theoretical pI of 7.85 and estimated mass of 34.8 kDa, with 76% identity to that from apple leaf (NCBI accession No. BAA01853). The sequence coding for *Ppe*Ald6PRase was subcloned into the pET19b vector and the recombinant enzyme was expressed with a His-tag at the N-terminus, in accordance with the strategy used for the apple leaf enzyme (Figueroa and Iglesias 2010), to obtain a protein of 333 amino acids and calculated mass of 37.4 kDa. The recombinant protein was recovered in the soluble fraction of transformed *Escherichia coli* cells and purified in a single step, resulting in a preparation with purity >95%, as assessed by densitometry of the scanned gel (**Supplementary Fig. S1**). Purified *Ppe*Ald6PRase migrated on gel filtration

Table 1 Kinetic parameters for the substrates of Ald6PRase from peach

Reaction	Substrate	K_m (mM)	V_{max} (U mg^{-1})
Glc-6P reduction	Glc-6P	11 ± 1	3.1 ± 0.1
	NADPH	0.031 ± 0.001	
Gol-6P oxidation	Gol-6P	3.5 ± 0.4	2.26 ± 0.07
	$NADP^+$	0.059 ± 0.006	

Reactions were performed as described in the Materials and Methods. Kinetic constants were calculated by fitting activity data to the Hill equation and using the mean of three independent data sets.

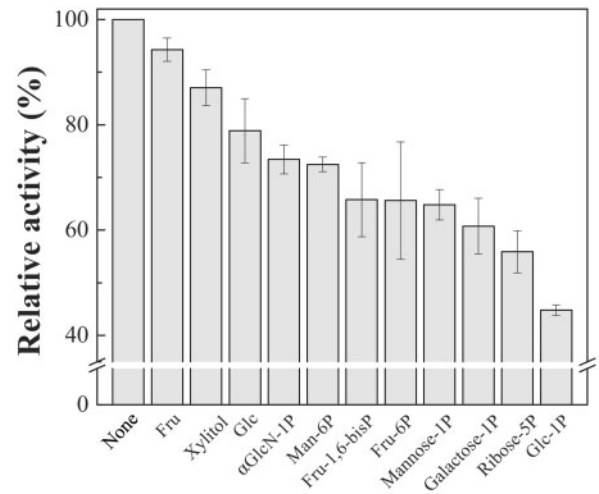

Fig. 2 Inhibition of peach Ald6PRase by metabolites. Activity was measured as described in the Materials and Methods in the presence of 20 mM Fru, xylitol, Glc, α-*N*-acetyl glucosamine-1P (αGlcN-1P), Man-6P, Fru-1,6-bisP, Fru-6P, Man-1P, galactose-1P, ribose-5P or Glc-1P. Activity values were normalized to the control without effectors. Values are the mean of three independent experiments ± SE.

chromatography as a protein of 67 kDa (**Supplementary Fig. S2**) and, based on the molecular mass of the monomer (~35 kDa; **Supplementary Fig. S1**), we estimated a dimeric quaternary structure.

We determined the kinetic parameters of the highly pure *Ppe*Ald6PRase in both directions of catalysis (**Table 1**). Kinetic constants were similar to those reported for the recombinant enzyme from apple leaf (Figueroa and Iglesias 2010) and other enzymes purified from their natural source (Hirai 1981, Negm and Loescher 1981, Kanayama and Yamaki 1993, Zhou et al. 2003b). We measured *Ppe*Ald6PRase activity using 20 mM Glc, Man-6P or ribose-5P as substrates; however, none of them was able to produce >3% of the activity obtained with 20 mM Glc-6P. Similarly, no activity was detected when NADPH and $NADP^+$ were replaced by NADH and NAD^+, respectively. No significant effects were observed when the activity of *Ppe*Ald6PRase was assayed in the presence of 5 mM Mg^{2+} or Ca^{2+} (data not shown).

We also investigated the effect of sugars and sugar-P on the activity of *Ppe*Ald6PRase. None of the effectors tested was able to activate the enzyme, whereas several inhibited its activity when assayed at 20 mM (**Fig. 2**). The strongest effect was observed for Glc-1P (~55% inhibition), while Fru-1,6-bisP, Fru-6P, mannose-1P, galactose-1P and ribose-5P all produced approximately 40% inhibition (**Fig. 2**). Hexoses (Glc and Fru) had little or no effect (**Fig. 2**), suggesting that the phosphate group plays a key role in inhibitor binding. Addition of a physiologically relevant concentration (100 μM) of trehalose-6P or Fru-2,6-bisP had no effect on *Ppe*Ald6PRase activity (data not shown).

To investigate further the inhibitory mechanism triggered by hexose-P, we measured Ald6PRase activity in the presence of fixed concentrations of each effector at varying concentrations of Glc-6P. All metabolites showed competitive inhibition relative to Glc-6P, with K_i values of 9.07, 26.0 and 55.4 mM for Glc-1P, Fru-1,6-bisP and Fru-6P, respectively (**Supplementary Fig. S3A–C**). Similar assays were performed with inorganic orthophosphate (Pi), previously shown to be an inhibitor of Ald6PRase from apple leaves (Zhou et al. 2003b). We also found that Pi is a competitive inhibitor relative to Glc-6P, with a K_i value of 29.6 mM (**Supplementary Fig. S3D**).

Ald6PRase purified from fully expanded apple leaves is completely inhibited by $AgNO_3$ (Negm and Loescher 1981), which directly interacts with sulfhydryl groups (Liau et al. 1997). Reactive oxygen or nitrogen species modify enzyme activity by affecting the oxidative state of thiols from cysteine residues, resulting in a modified protein with particular properties, depending on the species and concentration of the oxidant (Arias et al. 2010). *Ppe*Ald6PRase has three cysteine residues, which could be oxidized under stressful conditions (such as salinity, drought or cold, among others). In order to investigate the effect of an oxidative environment on enzyme activity, we incubated Ald6PRase in the presence of different ratios of 2-mercaptoethanol (2ME) to 2-hydroxyethyl disulfide (HEDS; the oxidized species of 2ME), producing a range of potentials (E_h) from −0.4 to 0 V. After redox equilibrium was achieved, we measured the remaining activity, which was close to 100% at electronegative potentials, whereas it was hardly detectable at values close to 0 V (**Fig. 3**). The inflexion point of the curve shown in **Fig. 3** (−0.237 V) is known as the midpoint potential (E_m), which represents the E_h value where 50% of the enzyme is inactivated. We also analyzed the effect of a physiological oxidizing molecule (hydrogen peroxide, H_2O_2) on *Ppe*Ald6PRase activity. Our results indicate that H_2O_2 oxidation causes enzyme inactivation in a time- and concentration-dependent manner (**Supplementary Fig. S4**), with a k'' of 0.033 ± 0.004 M^{-1} s^{-1}. These results suggest that an oxidizing environment diminishes Ald6PRase activity in vivo.

To explore further the redox effect on the functionality of *Ppe*Ald6PRase, we explored whether reducing agents could recover the activity of the oxidized protein. The enzyme was first treated with H_2O_2 and then incubated with either dithiothreitol (DTT) or peach TRX *h* (Hartman et al. 2014), but the activity could not be restored, indicating that this is an irreversible process (data not shown). Cysteine thiol groups can be oxidized to sulfenic acid, a reversible modification. These residues can be further oxidized to sulfinic and sulfonic acids, forms that cannot be reduced by DTT or TRX (Kiley and Storz

2004, Poole et al. 2004). Irreversible oxidation could produce a deleterious effect on enzyme structure. Thus, we analyzed the effect of oxidation on *Ppe*Ald6PRase solubility by incubating the enzyme with diamide (a relatively strong non-physiological oxidant) and measuring the absorbance of the resulting solution at 405 nm. Absorbance of the diamide-treated sample increased in a time-dependent manner, reaching a constant value at 60 min, while absorbance of the control (without diamide) remained relatively constant (**Supplementary Fig. S5A**). These results indicate that oxidation produces enzyme aggregation and insolubilization. Analysis by SDS–PAGE showed that the amount of enzyme in the insoluble fraction increased after 40 min in the treated samples, with a concomitant decrease of soluble *Ppe*Ald6PRase (**Supplementary Fig. S5B**). Similar results were obtained using H_2O_2 as the oxidizing molecule, although the increase in absorbance became constant after 6 h of treatment (**Supplementary Fig. S5C, D**).

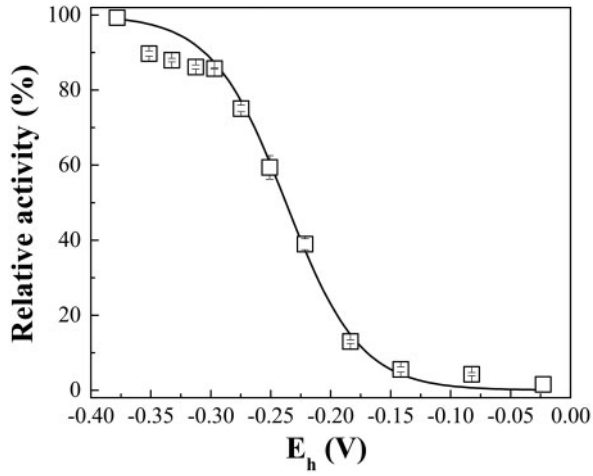

Fig. 3 Determination of the midpoint potential (E_m) for peach Ald6PRase. The enzyme was incubated with buffers containing different [2ME]/[HEDS] ratios until redox equilibrium was reached (1 h). Data of enzyme activity were normalized to the maximum value obtained within each assay and plotted vs. E_h. Values are the mean of three independent experiments ± SE.

We analyzed the effect of increasing the concentration of diamide on both *Ppe*Ald6PRase activity and solubility. Enzymatic activity decreased to approximately 7% at 500 μM diamide, with a maximum in absorbance at 405 nm (**Fig. 4A**). Analysis by SDS–PAGE of both soluble and insoluble fractions showed an enrichment of *Ppe*Ald6PRase in the insoluble fraction and the opposite pattern in the soluble fraction (**Fig. 4B**). When the samples treated with 500 μM diamide were analyzed by non-reducing SDS–PAGE, both the soluble and insoluble fractions showed the presence of high molecular mass aggregates of *Ppe*Ald6PRase (**Fig. 4C**, lanes 2 and 4), as confirmed by immunodetection of the protein bands (**Fig. 4D**, lanes 2 and 4). Moreover, the highly oxidized (mostly insolubilized) sample exhibited a wide range of bands (**Fig. 4D**, lane 4).

It has been reported that AKRases follow an ordered bi–bi reaction mechanism, with the cofactor binding first and leading to a conformational change in a particular loop (Davidson and Flynn 1979, Borhani et al. 1992, Kubiseski et al. 1992). We incubated *Ppe*Ald6PRase with diamide in the presence of $NADP^+$ or NAD^+ (which cannot be used as a substrate) to analyze whether these cofactors could protect the enzyme from insolubilization. **Fig. 5A** shows that NAD^+ reduced the turbidity rate, while $NADP^+$ completely protected the enzyme from insolubilization, maintaining the absorbance at values similar to those of the controls without diamide addition (**Fig. 5A**, inset). Analysis by SDS–PAGE showed that *Ppe*Ald6PRase remained entirely in the soluble fraction when incubated in the

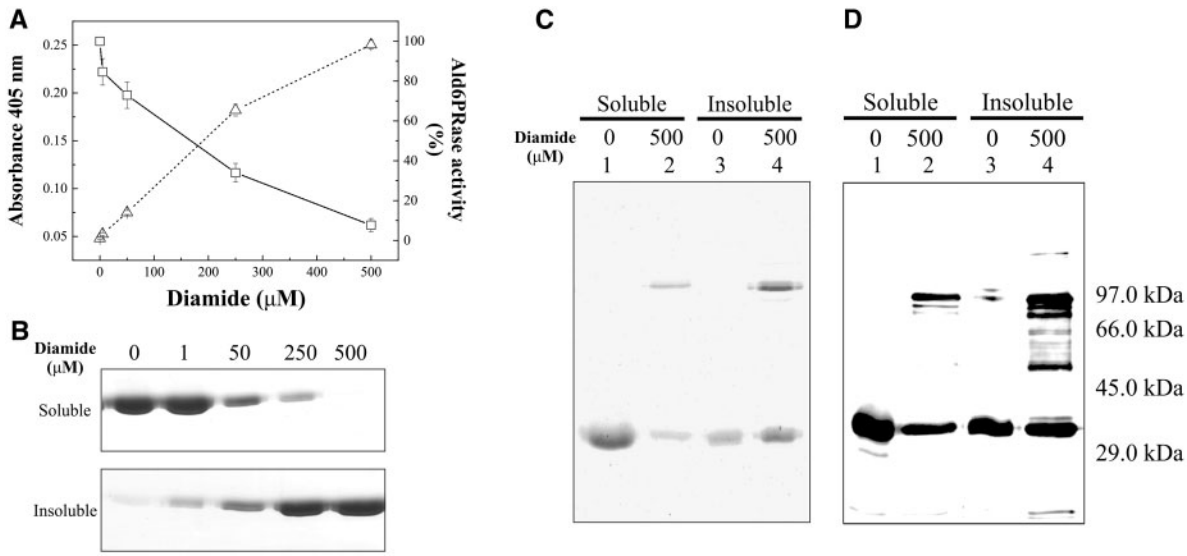

Fig. 4 Oxidation of peach Ald6PRase induces aggregation and enzyme inactivation. (A) Ald6PRase (5 μM) was incubated with concentrations of diamide ranging from 0 to 500 μM. After 1 h, the solution absorbance at 405 nm (dotted line) and Ald6PRase activity (continuous line) were measured. (B) All soluble and insoluble fractions from (A) were analyzed by reducing SDS–PAGE. Soluble and insoluble samples obtained after incubation with 0 and 500 μM diamide were subjected to non-reducing SDS–PAGE (C) followed by immunodetection with antibodies raised against apple Ald6PRase (D).

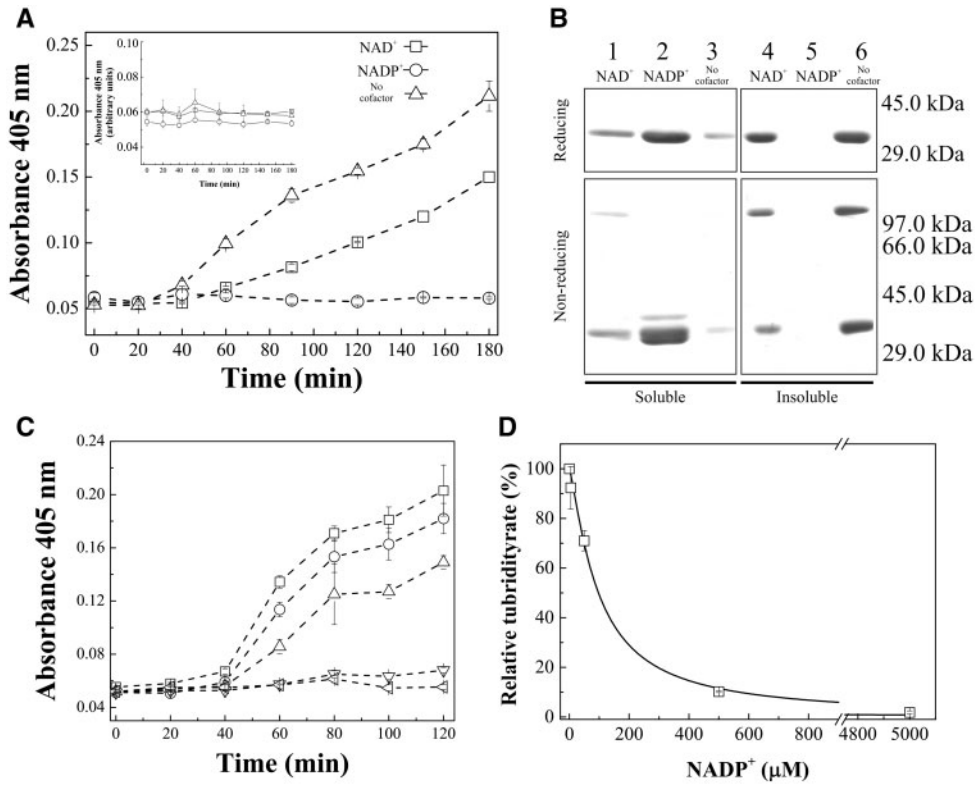

Fig. 5 $NADP^+$ protects peach Ald6PRase from oxidative insolubilization. (A) The enzyme (5 μM) was incubated with 250 μM diamide in the presence of 15 mM NAD^+ (open squares) or $NADP^+$ (open circles) and with no cofactor added (open triangles). The absorbance at 405 nm was measured over time. Inset: Ald6PRase incubated with or without cofactors in the absence of diamide. (B) After 180 min, soluble (left panels) and insoluble (right panels) fractions were separated and analyzed by reducing (upper panels) or non-reducing (bottom panels) SDS–PAGE. (C) The enzyme was incubated with diamide in the presence of different $NADP^+$ concentrations: 0 (open squares), 5 (open circles), 50 (upright triangles), 500 (inverted triangles) or 5,000 μM (horizontal triangles); and absorbance at 405 nm was measured over time. (D) Turbidity rates obtained from (C) were normalized to the value obtained without cofactor and plotted vs. $NADP^+$ concentration to calculate the K_d.

presence of $NADP^+$ (**Fig. 5B**, upper panels, lanes 2 and 5), while NAD^+ addition yielded similar amounts of enzyme in the insoluble fraction as the control (**Fig. 5B**, upper panels, lanes 4 and 6). Non-reducing SDS–PAGE revealed the existence of high molecular mass aggregates for the control and the sample incubated with NAD^+ (**Fig. 5B**, bottom panels, lanes 4 and 6), but not when the enzyme was incubated with $NADP^+$ (**Fig. 5B**, bottom panels, lane 5). Protection of the enzyme by $NADP^+$ was concentration dependent, with full protection occurring at concentrations of $\geq$500 μM (**Fig. 5C**). Furthermore, analysis of relative turbidity rates at different $NADP^+$ concentrations allowed us to calculate a K_d of 97 ± 19 μM (**Fig. 5D**), a value that is in the same order of the enzyme's K_m for the cofactor (**Table 1**).

Oxidized glutathione (GSSG) reacts with protein thiols to form protein–glutathione mixed disulfides in a process called glutathionylation or protein thiolation (Dalle-Donne et al. 2007, Rouhier et al. 2008). We analyzed the effect of 5 mM GSSG on *Ppe*Ald6PRase, but no significant changes in enzyme activity were observed after 4 h of treatment. To test if GSSG was capable of forming a mixed disulfide with the enzyme, we performed a labeling experiment with a conjugated di-eosin-glutathione disulfide (Di-E-GSSG). *Ppe*Ald6PRase was first incubated with GSSG or Di-E-GSSG. Then, samples were treated with Di-E-GSSG or DTT, respectively, and analyzed by non-reducing SDS–PAGE. Binding of Di-E-GSSG to *Ppe*Ald6PRase was thiol dependent, as DTT addition removed the label almost completely (**Fig. 6A**, lanes 4 and 5). The enzyme pre-treated with GSSG was also labeled with Di-E-GSSG, although to a lesser extent (58%) than the untreated protein (**Fig. 6A**, lanes 3 and 4). We then investigated if glutathionylation could protect cysteine thiols in *Ppe*Ald6PRase from irreversible modification. The enzyme was first incubated with 10 mM GSSG for 1 h and then treated with 50 μM diamide. As shown in **Fig. 6B**, the turbidity rate was 60% slower for the GSSG-pre-treated enzyme than the control. After 80 min, samples were centrifuged, and both soluble and insoluble fractions were analyzed by SDS–PAGE. The GSSG-pre-treated sample showed a lower amount of enzyme in the insoluble fraction than the control (data not shown).

Discussion

Enzymes from the AKRase superfamily catalyze a wide range of enzymatic reactions and are distributed across all kingdoms, from prokaryotes to animals (Hyndman et al. 2003). In plants,

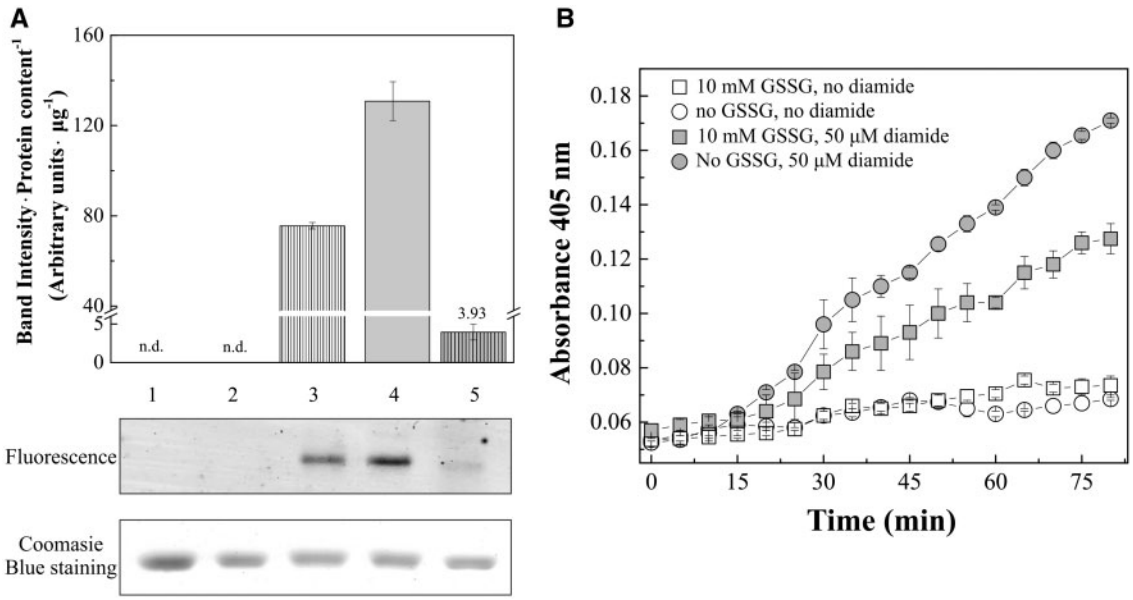

Fig. 6 Glutathionylation protects peach Ald6PRase from insolubilization. (A) The enzyme (5 µM) was incubated without redox agents (lane 1), with 150 µM GSSG (lane 2) or with 15 µM Di-E-GSSG (lane 4) for 1 h. After exhaustive washing, the sample pre-treated with GSSG was further incubated for 1 h with 15 µM Di-E-GSSG (lane 3), whereas the sample pre-treated with Di-E-GSSG was then incubated with 2.5 mM DTT (lane 5). Samples were analyzed by non-reducing SDS–PAGE. The amounts of protein loaded were 1 µg (lanes 1–5) for Coomasie Blue staining and 0.3 µg (lanes 1, 2 and 5) or 0.06 µg (lanes 3 and 4) for fluorescence detection. Band intensities were measured with ImageJ, and peak areas were normalized to the amount of protein loaded. (B) The enzyme (5 µM) was incubated for 1 h with 10 mM GSSG (squares) or without it (circles). The excess GSSG was removed by ultrafiltration, and samples were further treated with 50 µM diamide (gray symbols) or without it (open symbols).

AKRases play multiple roles, such as aldehyde detoxification, stress defense and synthesis of sugar alcohols and secondary metabolites (Sengupta et al. 2015). There are 12 well-defined groups in the AKRase superfamily. All sequences coding for plant AKRases analyzed so far fall within groups 2, 4 and 6. Enzymes from group 4 show a broad spectrum of activities so they were defined as multitasking soldiers (Sengupta et al. 2015). Conversely, members of group 2 seem to play a more defined role (i.e. synthesis of sugar alcohols). Yadav and Prasad (2014) performed a phylogenetic analysis of AKRases using representative sequences for each group. This allowed them to include Ald6PRase from rice in group 2 of the AKRase superfamily. Herein, we aimed to expand this group by using sequences with identity >60% to *Ppe*Ald6PRase. After data set curation, we ended up with 57 sequences, including rice and apple Al6PRases and celery Man6PRase (**Fig. 1**). Our tree shows that AKRases are present in very divergent families, from Selaginellaceae to Fabidae (**Fig. 1**). Proteins from peach, apple, pear and plum (which synthesize Gol) were clustered together, while Man6PRase from celery (a mannitol-synthesizing species) lies in a separate branch (**Fig. 1**). Interestingly, three sequences from rosaceous species (peach, apple and plum) were placed in a separate branch within the major group (**Fig. 1**). There are two genes encoding Ald6PRases in peach (Verde et al. 2013), and the number rises to 16 in apple (Velasco et al. 2010). We hypothesize that an ancient gene, already present in mosses (**Fig. 1**), was duplicated and specialized in species from the Rosaceae family to support Gol biosynthesis, while the common ancestor was kept to fulfill other roles.

Our work was focused on *Ppe*Ald6PRase, the isoform clustered within the branch containing most rosaceous Ald6PRases. The recombinant enzyme was purified to electrophoretic homogeneity and kinetically characterized (**Table 1**; **Supplementary Fig. S1**). We found that kinetic constants determined for recombinant *Ppe*Ald6PRase were similar to those from Ald6PRases purified from rosaceous (Hirai 1981, Negm and Loescher 1981, Kanayama and Yamaki 1993, Zhou et al. 2003b, Figueroa and Iglesias 2010) and non-rosaceous plants (Yadav and Prasad 2014). Both *Ppe*Ald6PRase (this work) and apple Ald6PRase (Figueroa and Iglesias 2010) are highly specific for Glc-6P and $NADP^+$. These enzymes show little or no activity with Man-6P, a C2 epimer of Glc-6P. Activity measurements and docking studies performed for rice Ald6PRase with its substrates (Glc-6P and Gol-6P) and Man-6P demonstrated that the latter can bind to the active center and generate hydrogen bonds with catalytic amino acids (Yadav and Prasad 2014). However, the carbonyl group in Man-6P is oriented in such a way that makes the *si* face available for hydride attack, while both Glc-6P and Gol-6P exposed their respective *re* face, providing a suitable explanation for the fact that Man-6P cannot be used as a substrate by any Ald6PRase studied so far (Figueroa and Iglesias 2010, Yadav and Prasad 2014).

It has been reported that Mg^{2+} activates Ald6PRase purified from apple leaves by lowering the K_m for Glc-6P from 9.8 to

5.1 mM (Zhou et al. 2003b). However, in our hands, Mg^{2+} did not produce any particular effect on the activity of *Ppe*Ald6PRase or recombinant apple Ald6PRase (unpublished results). Although the activation reported by Zhou et al. (2003b) is moderate, we do not discard the possibility that the enzyme purified from the natural source could harbor post-translational modifications (absent in our recombinant proteins), which might be important for enzyme regulation.

We found that different sugar-Ps inhibited *Ppe*Ald6PRase (**Fig. 2**), and detailed inhibition kinetics showed that Glc-1P, Fru-1,6-bisP and Fru-6P acted as competitive inhibitors with respect to Glc-6P (**Supplementary Fig. S3A–C**). Despite the fact that these metabolites inhibit the enzyme in vitro, the calculated K_i values are considerably high. We estimate that concentrations of Glc-6P and Fru-6P are approximately 9.5 and 2.6 mM, respectively. This assumption is based on metabolite levels reported for apple leaves (Cheng et al. 2005) and the cytosolic volume of mesophyll cells from peach leaves (Nadwodnik and Lohaus 2008). Unfortunately, we could not find data for Glc-1P and Fru-1,6-bisP from rosaceous species. Our estimate for Glc-6P is close to the K_m of recombinant Ald6PRases from apple (Figueroa and Iglesias 2010) and peach (this work) leaves, as well as those previously reported for enzymes purified from their natural source (Hirai 1981, Negm and Loescher 1981, Kanayama and Yamaki 1993, Zhou et al. 2003b). However, the K_i for Fru-6P is 20-fold higher than its estimated cytosolic concentration. Thus, the role of sugar-P in the regulation of Ald6PRase in vivo remains to be elucidated.

Also, Pi acted as a competitive inhibitor with respect to Glc-6P, with a K_i value of 29.6 mM (**Supplementary Fig. S3D**). It has been reported that Pi is a mixed inhibitor with respect to Glc-6P (K_i of 0.42 mM) of Ald6PRase purified from fully developed apple leaves (Zhou et al. 2003b). Different reasons could explain such differences. For instance, the enzyme purified from plant tissues could be regulated at the post-translational level, which might modify the enzyme's susceptibility to regulators (Echeverria et al. 1994, Feria et al. 2008). A good example is phosphorylation of Ser158 in sucrose-6P synthase from spinach leaves, which alters the affinity for Fru-6P (one of the substrates) and its susceptibility to the activator (Glc-6P) and the inhibitor (Pi), with no visible changes in the V_{max} (Toroser et al. 1998). Additionally, Ald6PRase belongs to a multigenic family (Velasco et al. 2010, Verde et al. 2013), and the resulting isoforms could have different sensitivity to metabolites and be expressed in different stages of plant development or tissues. Nevertheless, Pi could play an important role on the regulation of Gol synthesis. Cytosolic Pi levels are directly related to the photosynthetic rate (Rychter et al. 2016). Export of triose-P from the chloroplast during the photoperiod decreases cytosolic Pi levels, which in turn could promote Gol synthesis not only by alleviating Pi inhibition of Ald6PRase but also by providing the substrate for Gol synthesis (Glc-6P). The opposite occurs in the dark period: export of triose-P decreases, Pi import into the chloroplast is reduced, and thus its levels in the cytosol increase, leading to inhibition of Ald6PRase. This putative scenario fits well with data from peach leaves showing that Gol levels peak around noon and decrease during the night (Li et al. 2007).

It was previously suggested that cysteine residues could participate in the regulation of apple Ald6PRase (Negm and Loescher 1981, Zhou et al. 2003b), but detailed redox studies on a plant Ald6PRase have never been carried out until now. We determined that the redox environment influences *Ppe*Ald6PRase activity, with electronegative potentials favoring enzyme activity and vice versa (electropositive potentials produced a marked decrease in enzyme activity; **Fig. 3**). Incubation with H_2O_2 irreversibly inactivated the enzyme, probably by oxidation of cysteine thiols to sulfinic or sulfonic acids, oxidation states that cannot be reverted by TRX or DTT (Kiley and Storz 2004, Poole et al. 2004). Similar results were reported for human AKR1B10, which showed a significant decrease of its free sulfhydryl groups and lower enzymatic activity when exposed to reactive oxygen species mixtures (Shen et al. 2010).

The k'' for *Ppe*Ald6PRase inactivation by H_2O_2 was 0.033 M^{-1} s^{-1}, a value considerably lower than those reported for other redox-regulated enzymes, such as np-Ga3PDHase and Ga3PDHase (EC 1.2.1.12) from wheat (1.9 and 115 M^{-1} s^{-1}, respectively) (Piattoni et al. 2013) or peach GolDHase (6.9 M^{-1} s^{-1}) (Hartman et al. 2014). These results suggest that *Ppe*Ald6PRase is quite resistant to oxidation; however, the enzyme showed destabilization and insolubilization after incubation with relatively high concentrations of diamide and H_2O_2 (0.5 mM) for considerably long time periods (1 and 6 h, respectively) (**Fig. 4**; **Supplementary Fig. S5**). Protein destabilization and insolubilization as a consequence of exposure to oxidative environments have been described for both plant (Piattoni et al. 2013) and human (Li et al. 1995) proteins. In vivo studies demonstrated that protease activity is induced under stress conditions within plant cells to process protein aggregates (Pena et al. 2006). Furthermore, under extreme oxidative damage, these aggregates could be processed by the autophagic pathway (Thompson and Vierstra 2005, Patel et al. 2006), which is rapidly induced by stress (Xiong et al. 2007). Whether oxidized *Ppe*Ald6PRase is degraded in vivo by these mechanisms remains to be investigated.

Incubation of *Ppe*Ald6PRase with NAD^+ diminished the enzyme's turbidity rate, whereas $NADP^+$ completely prevented its precipitation, as was previously reported for Gol dehydrogenase from rat liver (Kanda et al. 2012). The protection exerted by the physiological cofactor could be relevant under oxidizing conditions in planta. We also found that *Ppe*Ald6PRase could be glutathionylated in vitro, a process reversible by incubation with DTT (**Fig. 6A**). Glutathionylation of *Ppe*Ald6PRase did not affect enzymatic activity but diminished the turbidity rate under severe oxidative conditions (**Fig. 6B**). Glutathionylation of human AKRases (AKR1C1 and AKR1C3) was recently reported (Lu et al. 2015), although no physiological function was attributed to such a modification. Reversible glutathionylation could play an essential role protecting the enzyme against oxidative environments. Protein mixed disulfides engage protein thiols in the cell antioxidant defense machinery and, at the same time, protect them from irreversible oxidation (Rouhier et al. 2004).

The NADPH used for polyol synthesis in plants mainly comes from the irreversible oxidation of Ga3P by the cytosolic

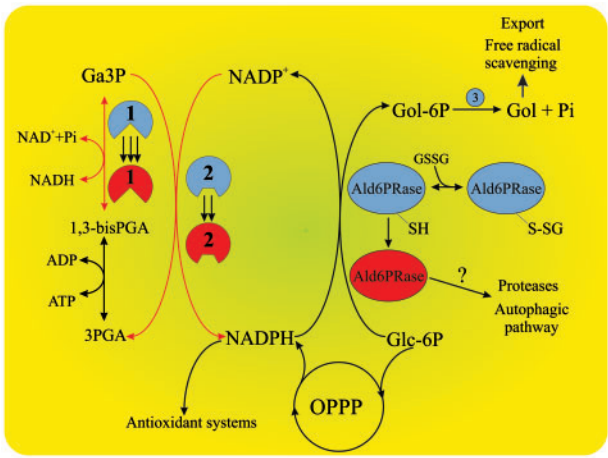

Fig. 7 Proposed model for the redox regulation of peach Ald6PRase. Under a stress situation, Ga3PDHase (1) is rapidly inactivated and carbon flux is directed towards the alternative route catalyzed by np-Ga3PDHase (2), increasing the synthesis of NADPH necessary to support Gol synthesis by Ald6PRase, which is more resistant to oxidation. Gol could act as a free radical scavenger not only in photosynthetic cells but also in heterotrophic tissues. If oxidative conditions persist, both Ga3PDHase and np-Ga3PDHase are inactivated. Glutathionylation could protect Ald6PRase from aggregation, thus maintaining Gol synthesis. If Ald6PRase is inactivated, Gol synthesis stops and NADPH would be available for other reactions. Moreover, in this case, Glc-6P would be used to feed the oxidative pentose-P pathway (OPPP) to keep NADPH supply for other antioxidant systems. Irreversibly inactivated Ald6PRase could be degraded either by proteases or by the autophagic pathway. The sensitivity of enzymes to oxidation is denoted by the number of arrows: three, high; two, medium; one, low. Black arrows, reactions occurring even under oxidative stress; red arrows, reactions inhibited under stress situations. Blue, active enzymes; red, inactive enzymes. (3) Gol-6P phosphatase.

np-Ga3PDHase (Rumpho et al. 1983, Gao and Loescher 2000), an alternative step to the reversible reaction catalyzed by Ga3PDHase (Figueroa et al. 2016). Under oxidative conditions, the latter is rapidly inactivated and insolubilized, whereas the former is more resistant to oxidation (Piattoni et al. 2013). Then, carbon flux is directed to the alternative pathway to generate reducing power (NADPH) to support antioxidant systems. It is worth mentioning that putative np-Ga3PDHase and Ga3PDHase from peach show an identity >80% with the enzymes from wheat. Moreover, the cysteine residues that might be involved in the redox regulation of wheat enzymes are highly conserved (data not shown). Based on the k'' values, *Ppe*Ald6PRase seems to be even more resistant than np-Ga3PDHase to H_2O_2 oxidation (see above). As previously mentioned, sugar alcohols have multiple roles against oxidative stress, including free radical scavenging. Based on our results, it is tempting to speculate that Gol production would be maintained even under oxidizing conditions (**Fig. 7**).

Del Corso et al. (1994) proposed a model of concerted enzymatic activities capable of generating a defense system which acts as the last antioxidant barrier within cells. Both oxidation and glutathionylation of enzymes would be linked to NADPH homeostasis by maximizing its synthesis (through the oxidative pentose-P pathway) and decreasing its consumption (by inactivation of the enzymes using the reduced cofactor). We suggest that carbon flux into Gol synthesis would be decreased only under extended perturbations of the physiological redox state as a consequence of Ald6PRase inactivation, a process that could be attenuated by enzyme thiolation (**Fig. 7**). The levels of sugar alcohols increase when plants are exposed to cold (Williams and Raese 1974, Hirai 1983, Loescher et al. 1990), drought (Ranney et al. 1991) and salinity (Everard et al. 1994, Gao et al. 2001, Pommerrenig et al. 2007). However, Gol synthesis might play a secondary role under extreme oxidative situations, when Ald6PRase would be inactivated to reduce utilization of NADPH, necessary to keep antioxidant systems fully functional (**Fig. 7**). Moreover, Glc-6P not used for Gol synthesis could feed the oxidative pentose-P pathway to generate even more NADPH (Del Corso et al. 1994).

Results presented in this work indicate that Ald6PRase is finely regulated by metabolites and post-translational modifications, reinforcing our previous knowledge and providing new insights into the regulation of Gol biosynthesis.

Materials and Methods

Plant material, bacterial strains and reagents

Mature leaves from peach (*Prunus persica* cv. Flordaking) trees were harvested at EEA San Pedro (INTA, Buenos Aires, Argentina), rapidly frozen with liquid N_2 and stored at −80°C until use. *Escherichia coli* TOP10 cells (Invitrogen) were used for cloning procedures and plasmid maintenance. Protein expression was carried out using *E. coli* BL21 Star (DE3) cells (Invitrogen). The substrates used to determine enzyme activity were from Sigma. All other reagents were of the highest purity available.

Phylogenetic analysis

Using the sequence coding for *Ppe*Ald6PRase (NCBI accession No. EF576940.2) as query, we obtained 67 plant sequences from Phytozome v9.1 (http://www.phytozome.org/), NCBI (http://www.ncbi.nlm.nih.gov/) and the GDR database (https://www.rosaceae.org/). Sequences with identity <60% to *Ppe*Ald6PRase and those lacking putative catalytic amino acids (Jez et al. 1997, Kratzer et al. 2006) were manually discarded. The remaining 57 sequences (**Supplementary Dataset S1**) were aligned in Clustal Omega (http://www.ebi.ac.uk/Tools/msa/clustalohttp://www.ebi.ac.uk/Tools/msa/clustalo/). We used SeaView 4.6 (Gouy et al. 2010) to build the phylogenetic tree using the Neighbor–Joining algorithm, with a bootstrap value of 10,000. **Fig. 1** was prepared using FigTree 1.4.2 (http://tree.bio.ed.ac.uk/software/figtree/).

Cloning of the sequence coding for *Ppe*Ald6PRase

Total RNA from peach leaves was isolated using Trizol (Invitrogen). cDNA was synthesized at 42°C for 1 h in a 2 µl reaction mixture containing 0.25 µg of RNA, 200 pmol of oligo(dT) primer and 200 U of M-MLV reverse transcriptase (USB). To amplify the gene coding for *Ppe*Ald6PRase, we designed the primers *Ppe*Ald6PRase-fo (CATATGTCCACCATAACTCTCAACAATG, the *Nde*I site is underlined) and *Ppe*Ald6PRase-re (GTCGACTGCATAAACATCTACTCCCC, the *Sal*I site is underlined), based on the sequence coding for *Prunus salicina* Ald6PRase (NCBI accession No. FJ645737.1).

Amplifications by PCR were performed with 1 µl of cDNA solution, 100 pmol of each primer and 2.5 U of *Taq* DNA polymerase (Fermentas), with the following conditions: 5 min at 95°C, 30 cycles of 1 min at 95°C, 30 s at 50°C and 1 min 30 s at 72°C, followed by 10 min at 72°C. DNA fragments were cloned into the pGEM-T Easy vector (Promega) and the resulting constructions were used to transform *E. coli* TOP10 cells. The sequences of the

amplified genes were confirmed by automated sequencing of two different clones (Macrogen). This sequence was subcloned into the pET19b vector (Novagen) between *Nde*I and *Xho*I sites to obtain the recombinant protein linked to a His-tag at the N-terminus.

Protein expression and purification

The construct [pET19b/*Ppe*Ald6PRase] was used to transform *E. coli* BL21 Star (DE3) cells. Expression of *Ppe*Ald6PRase was achieved by inoculating 1 liter of LB mediaum (supplemented with 100 μg ml^{-1} ampicillin) with a 1/100 dilution of an overnight culture. Cells were grown at 37°C and 200 r.p.m. in an orbital shaker until the OD_{600} reached approximately 0.6, induced with 0.2 mM isopropyl-β-D-thiogalactopyranoside (IPTG) at 25°C overnight, harvested at 5,000 × *g* at 4°C for 15 min and kept at −20°C until use.

The cell paste was resuspended with 20 ml of Buffer H [25 mM Tris–HCl pH 8.0, 5% (v/v) glycerol, 10 mM imidazole] and disrupted by sonication. The resulting suspension was centrifuged twice at 35,000 × *g* at 4°C for 15 min and the supernatant was loaded in a 1 ml HisTrap column (GE Healthcare) connected to an ÄKTA Explorer 100 purification system (GE Healthcare) previously equilibrated with Buffer H. After sample loading, the column was washed with 10 ml of Buffer H and the recombinant protein was eluted with a linear gradient of imidazole (10–300 mM, 50 ml). Fractions of 2 ml were collected, and those containing the enzyme of interest were pooled and concentrated. The proteins were aliquoted, stored at −80°C and thawed only once just before use. Under these conditions, the proteins were stable and remained active for at least 6 months.

Protein methods

Protein electrophoresis was carried out under denaturing conditions (SDS–PAGE) as described by Laemmli (1970). Non-reducing SDS–PAGE was performed by preparing samples with sample buffer without reducing agent. Protein band intensities were evaluated by densitometry using the ImageJ 1.50i program (Abràmoff et al. 2004). Protein concentration was determined following the procedure described by Bradford (1976) using bovine serum albumin (BSA) as standard.

Native molecular mass determination

The native molecular mass of *Ppe*Ald6PRase was determined using a Superdex 200 5/200 Tricorn column (GE Healthcare) equilibrated with 50 mM HEPES pH 8.0. A calibration curve was constructed by plotting the elution volume vs. $\log_{10}$ of the molecular mass from standard proteins (ovalbumin, 43 kDa; conalbumin, 75 kDa; aldolase, 158 kDa; ferritin, 440 kDa; and thyroglobulin, 669 kDa).

Enzyme activity assay and determination of kinetic constants

The activity of *Ppe*Ald6PRase was determined as previously described for recombinant apple Ald6PRase (Figueroa and Iglesias 2010). In the direction of Glc-6P reduction, the standard assay mixture contained 100 mM Tris–HCl pH 8.0, 0.2 mM NADPH, 25 mM Glc-6P and the proper amount of enzyme. In the direction of Gol-6P oxidation, the standard medium composition was 100 mM Tris–HCl pH 8.0, 1 mM $NADP^+$, 20 mM Gol-6P and enzyme at an appropriate dilution. Both reactions were carried out in a final volume of 50 μl at 25°C in a Multiskan Ascent 384-microplate reader (Thermo Electron Corporation). One unit of enzyme activity (U) is defined as the amount of enzyme catalyzing the reduction/oxidation of 1 μmol $NADP^+$/NADPH in 1 min under the specified assay conditions.

Data of initial velocity (v) were plotted vs. substrate concentration, and kinetic constants were calculated by fitting to the Michaelis–Menten equation: $v = V_{max}\,S/(K_m + S)$, where K_m is the substrate concentration (S) producing 50% of the maximal velocity (V_{max}). Fitting was performed by a non-linear least-squares algorithm provided by the computer program Origin 8.0 (OriginLab Corporation). Kinetic constants were determined using the mean of three independent data sets, reproducible within ±10%.

Redox assays

Recombinant *Ppe*Ald6PRase was incubated with redox agents at 25°C with 25 mM Tris–HCl pH 8.0 and 5% (v/v) glycerol. Aliquots were taken from the reaction mixtures at regular time intervals and assayed for activity in the direction of Glc-6P reduction. To remove the excess oxidizing compounds prior to addition of reducing agents, the enzyme was ultrafiltrated by centrifuging at 10,000 × *g* and 4°C using a Vivaspin 500 device (Sartorius). To analyze the oxidation kinetics of *Ppe*Ald6PRase, we utilized the model of irreversible inhibition of enzymes described by Kitz and Wilson (1962), as we previously did for GolDHase from peach fruits (Hartman et al. 2014).

Determination of the midpoint reduction potential

The E_m of a protein is defined as the reduction potential in which the concentrations of oxidized and reduced proteins are equal (Schafer and Buettner 2001). The E_m of *Ppe*Ald6PRase was determined by redox titration with 2ME-HEDS, following the protocol described for peach fruits GolDHase (Hartman et al. 2014). *Ppe*Ald6PRase (5 μM) was incubated for 1 h at 25°C in different redox buffers (redox equilibrium was reached; data not shown). Aliquots of treated samples were taken and enzyme activity was assayed in the direction of Glc-6P reduction under standard conditions (see above). Data of *Ppe*Ald6PRase activity were plotted vs. E and fitted using the program Origin 8.0 to the Nernst equation: $E = E_m - RT/nF\ \ln([2ME]^2/[HEDS])$, to calculate the E_m.

Turbidity assays

Turbidity measurements, used as a proxy for protein aggregation, were performed in a flat-bottom 96-well microtiter plate (Corning). Recombinant *Ppe*Ald6PRase was treated with diamide or H_2O_2 in 100 mM Tris–HCl pH 8.0, 300 mM NaCl, and 5% (v/v) glycerol at 25°C, and aliquots were taken at different times. The enzyme incubated in the same buffer but without oxidant was used as control. Turbidity of samples was followed by measuring the absorbance at 405 nm in a microplate reader (Nakajima et al. 2007). Immediately after the turbidity measurement, samples were centrifuged 20 min at 14,000 × *g* and 4°C to separate the soluble and insoluble fractions. All samples were subjected to SDS–PAGE in reducing or non-reducing conditions, depending on the assay. The turbidity rate was calculated by fitting the data of turbidity vs. time to a linear equation. These values were plotted as a function of $NADP^+$ concentration and fitted using the following equation: $t = t_0 + (T_{min} - t_0) \times [NADP^+]/(K_d + [NADP^+])$, where t is the turbidity rate, t_0 is the turbidity rate without $NADP^+$, T_{min} is the minimum turbidity rate and K_d is the dissociation constant for $NADP^+$.

Glutathionylation and Di-E-GSSG labeling

Assays were performed as previously described by Bräutigam et al. (2013), with minor modifications. *Ppe*Ald6PRase (5 μM) was incubated with either 150 μM GSSG (10 : 1 GSSG : enzyme thiols) or 15 μM Di-E-GSSG (1 : 1 Di-E-GSSG : enzyme thiols; Cayman Chemical Company) for 60 min at 25°C in a medium containing 100 mM Tris–HCl pH 8.0 and 5% (v/v) glycerol. The excess GSSG and Di-E-GSSG was removed by ultrafiltration (as described earlier). Then, the GSSG-treated sample was incubated with 15 μM Di-E-GSSG, while the Di-E-GSSG-treated sample was incubated with 2.5 mM DTT (treatments were performed for 60 min at 25°C). As a control, Ald6PRase was kept at the same temperature in the reaction media without redox agents for 2 h. Finally, samples were analyzed by non-reducing SDS–PAGE. The fluorescence corresponding to Di-E-gluthationylated proteins was measured using a Typhoon 9400 scanner (GE Healthcare; excitation wavelength 532 nm and emission wavelength 555 nm). After scanning, gels were stained with Coomasie Brilliant Blue.

Production of antibodies and immunodetection

Antibodies against Ald6PRase from apple (*Malus domestica*) leaves (Figueroa and Iglesias 2010) were raised in rabbits immunized with the purified recombinant protein, as previously described (Vaitukaitis et al. 1971). After SDS–PAGE, proteins were transferred to nitrocellulose membranes at 180 mA for 60 min. Membranes were incubated for 1 h at 25°C with rabbit anti-Ald6PRase diluted 1/1,000. Membranes were washed and incubated with anti-rabbit IgG conjugated to Alexa Fluor 647 (Invitrogen). Emission signal was detected using a Typhoon 9400 scanner (GE Healthcare).

Supplementary data

Supplementary data are available at PCP online.

Funding

This work was supported by the Agencia Nacional de Promoción Científica y Tecnológica [PICT-2014–1305 to C.M.F. and PICT-2014-3256 to A.A.I.]; Universidad Nacional del Litoral [CAI+D 2011 to A.A.I.]; and Consejo Nacional de Investigaciones Científicas y Técnicas [PIO CONICET-YPF 13320140100061CO to A.A.I.].

Acknowledgments

We thank Luis Arroyo (EEA San Pedro, INTA, Argentina) for providing peach leaves. M.D.H. is a Postdoctoral Fellow from CONICET; C.M.F., D.G.A. and A.A.I. are Researchers from the same institution.

Disclosures

The authors have no conflicts of interest to declare.

References

Abràmoff, M.D., Magalhães, P.J. and Ram, S.J. (2004) Image processing with imageJ. *Biophotonics* 11: 36–41.

Arias, D.G., Piattoni, C.V., Guerrero, S.A. and Iglesias, A.A. (2010) Biochemical mechanisms for the maintenance of oxidative stress under control in plants. *In* Handbook of Plant and Crop Stress, 3rd edn. Edited by Pessarakli, M. pp.157–190. CRC Press, Boca Raton, FL.

Ballicora, M.A., Iglesias, A.A. and Preiss, J. (2004) ADP-glucose pyrophosphorylase: a regulatory enzyme for plant starch synthesis. *Photosynth. Res.* 79: 1–24.

Borhani, D.W., Harter, T.M. and Petrash, J.M. (1992) The crystal structure of the aldose reductase·NADPH binary complex. *J. Biol. Chem.* 267: 24841–24847.

Bradford, M.M. (1976) A rapid and sensitive method for the quantitation of microgram quantities of protein using the principle of protein–dye binding. *Anal. Biochem.* 72: 248–254.

Bräutigam, L., Jensen, L.D.E., Poschmann, G., Nyström, S., Bannenberg, S., Dreij, K., et al. (2013) Glutaredoxin regulates vascular development by reversible glutathionylation of sirtuin 1. *Proc. Natl. Acad. Sci. USA* 110: 20057–20062.

Cheng, L., Zhou, R., Reidel, E.J., Sharkey, T.D. and Dandekar, A.M. (2005) Antisense inhibition of sorbitol synthesis leads to up-regulation of starch synthesis without altering CO_2 assimilation in apple leaves. *Planta* 220: 767–776.

Del Corso, A., Cappiello, M. and Mura, U. (1994) Thiol dependent oxidation of enzymes: the last chance against oxidative stress. *Int. J. Biochem.* 26: 745–750.

Dalle-Donne, I., Rossi, R., Giustarini, D., Colombo, R. and Milzani, A. (2007) S-glutathionylation in protein redox regulation. *Free Radic. Biol. Med.* 43: 883–898.

Davidson, W.S. and Flynn, T.G. (1979) Kinetics and mechanism of action of aldehyde reductase from pig kidney. *Biochem. J.* 177: 595–601.

Echeverria, C., Pacquit, V., Bakrim, N., Osuna, L., Delgado, B., Arrio-Dupont, M., et al. (1994) The effect of pH on the covalent and metabolic control of C_4 phospho*enol*pyruvate carboxylase from *Sorghum* leaf. *Arch. Biochem. Biophys.* 315: 425–430.

Everard, J.D., Gucci, R., Kann, S.C., Flore, J.A. and Loescher, W.H. (1994) Gas-exchange and carbon partitioning in the leaves of celery (*Apium graveolens* L) at various levels of root-zone salinity. *Plant Physiol.* 106: 281–292.

Feria, A.-B., Alvarez, R., Cochereau, L., Vidal, J., García-Mauriño, S. and Echevarría, C. (2008) Regulation of phospho*enol*pyruvate carboxylase phosphorylation by metabolites and abscisic acid during the development and germination of barley seeds. *Plant. Physiol.* 148: 761–774.

Figueroa, C.M. and Iglesias, A.A. (2010) Aldose-6-phosphate reductase from apple leaves: importance of the quaternary structure for enzyme activity. *Biochimie* 92: 81–88.

Figueroa, C.M., Piattoni, C.V., Trípodi, K., Podestá, F.E. and Iglesias, A.A. (2016) Carbon photoassimilation and photosynthate partitioning in plants. *In* Handbook of Photosynthesis, 3rd edn. Eddited by Pessarakli, M.. pp. 509–535. CRC Press, Boca Raton, FL.

Gao, Z. and Loescher, W.H. (2000) NADPH supply and mannitol biosynthesis. Characterization, cloning, and regulation of the dehydrogenase in celery leaves. *Plant Physiol.* 124: 321–330.

Gao, M., Tao, R., Miura, K., Dandekar, A.M. and Sugiura, A. (2001) Transformation of Japanese persimmon (*Diospyros kaki* Thunb.) with apple cDNA encoding NADP-dependent sorbitol-6-phosphate dehydrogenase. *Plant Sci.* 160: 837–845.

Gouy, M., Guindon, S. and Gascuel, O. (2010) SeaView version 4: a multiplatform graphical user interface for sequence alignment and phylogenetic tree building. *Mol. Biol. Evol.* 27: 221–224.

Hartman, M.D., Figueroa, C.M., Piattoni, C.V. and Iglesias, A.A. (2014) Glucitol dehydrogenase from peach (*Prunus persica*) fruits is regulated by thioredoxin *h*. *Plant Cell Physiol.* 55: 1157–1168.

Hayat, S., Hayat, Q., Alyemeni, M.N., Wani, A.S., Pichtel, J. and Ahmad, A. (2012) Role of proline under changing environments: a review. *Plant Signal. Behav.* 7: 1456–1466.

Hirai, M. (1981) Purification and characteristics of sorbitol-6-phosphate dehydrogenase from loquat leaves. *Plant Physiol.* 67: 221–224.

Hirai, M. (1983) Seasonal changes in sorbitol-6-phosphate dehydropenase in loquat leaf. *Plant Cell Physiol.* 24: 925–931.

Hsiao, T.C., Acevedo, E., Fereres, E. and Henderson, D.W. (1976) Water stress, growth, and osmotic adjustment. *Philos. Trans. R. Soc. B: Biol. Sci.* 273: 479–500.

Hyndman, D., Bauman, D.R., Heredia, V.V. and Penning, T.M. (2003) The aldo-keto reductase superfamily homepage. *Chem. Biol. Interact.* 143–144: 621–631.

Jez, J.M., Bennett, M.J., Schlegel, B.P., Lewis, M. and Penning, T.M. (1997) Comparative anatomy of the aldo-keto reductase superfamily. *Biochem. J.* 326: 625–636.

Kanayama, Y. and Yamaki, S. (1993) Purification and properties of NADP-dependent sorbitol-6-phosphate dehydrogenase from apple seedlings. *Plant Cell Physiol.* 34: 819–823.

Kanda, H., Toyama, T., Shinohara-Kanda, A., Iwamatsu, A., Shinkai, Y., Kaji, T., et al. (2012) S-Mercuration of rat sorbitol dehydrogenase by methylmercury causes its aggregation and the release of the zinc ion from the active site. *Arch. Toxicol.* 86: 1693–1702.

Kiley, P.J. and Storz, G. (2004) Exploiting thiol modifications. *PLoS Biol.* 2: e400.

Kitz, R. and Wilson, I.B. (1962) Esters of methanesulfonic acid as irreversible inhibitors of acetylcholinesterase. *J. Biol. Chem.* 237: 3245–3249.

Kratzer, R., Wilson, D.K. and Nidetzky, B. (2006) Catalytic mechanism and substrate selectivity of aldo-keto reductases: insights from structure–function studies of *Candida tenuis* xylose reductase. *IUBMB Life* 58: 499–507.

Kubiseski, T.J., Hyndman, D.J., Morjana, N.A. and Flynn, T.G. (1992) Studies on pig muscle aldose reductase. Kinetic mechanism and evidence for a slow conformational change upon coenzyme binding. *J. Biol. Chem.* 267: 6510–6517.

Laemmli, U.K. (1970) Cleavage of structural proteins during the assembly of the head of bacteriophage T4. *Nature* 227: 680–685.

Li, S., Nguyen, T.H., Schöneich, C. and Borchardt, R.T. (1995) Aggregation and precipitation of human relaxin induced by metal-catalyzed oxidation. *Biochemistry* 34: 5762–5772.

Li, W.D., Duan, W., Fan, P.G., Yan, S.T. and Li, S.H. (2007) Photosynthesis in response to sink–source activity and in relation to end products and activities of metabolic enzymes in peach trees. *Tree Physiol.* 27: 1307–1318.

Liau, S.Y., Read, D.C., Pugh, W.J., Furr, J.R. and Russell, A.D. (1997) Interaction of silver nitrate with readily identifiable groups: relationship to the antibacterial action of silver ions. *Lett. Appl. Microbiol.* 25: 279–283.

Loescher, W.H. and Everard, J.D. (2004) Regulation of sugar alcohol biosynthesis. *In* Photosynthesis: Physiology and Metabolism. Edited by Leegood, R.C., Sharkey, T.D. and von Caemmerer, S. pp.275–299. Kluwer Academic Publishers, Dordrecht, The Netherlands.

Loescher, W.H., Marlow, G.C. and Kennedy, R.A. (1982) Sorbitol metabolism and sink–source interconversions in developing apple leaves. *Plant Physiol.* 70: 335–339.

Loescher, W.H., McCamant, T. and Keller, J.D. (1990) Carbohydrate reserves, translocation, and storage in woody plant roots. *HortScience* 25: 274–281.

Lu, S., Fan, S.-B., Yang, B., Li, Y.-X., Meng, J.-M., Wu, L., et al. (2015) Mapping native disulfide bonds at a proteome scale. *Nat. Methods* 12: 329–331.

MacRae, E. and Lunn J.E. (2012) Photosynthetic sucrose biosynthesis: an evolutionary perspective. *In* Photosynthesis: Plastid Biology, Energy Conversion and Carbon Assimilation. Edited by Eaton-Rye, J.J., Tripathy, B.C. and Sharkey, T.D. pp.675–702. Springer, Dordrecht, The Netherlands.

Moing, A. (2000) Sugar alcohols as carbohydrate reserves in some higher plants. *In* Carbohydrate Reserves in Plants—Synthesis and Regulation. Edited by Gupta, A.K. and Kaur, N. pp.337–358. Elsevier, Amsterdam.

Nadwodnik, J. and Lohaus, G. (2008) Subcellular concentrations of sugar alcohols and sugars in relation to phloem translocation in *Plantago major*, *Plantago maritima*, *Prunus persica*, and *Apium graveolens*. *Planta* 227: 1079–1089.

Nakajima, H., Amano, W., Fujita, A., Fukuhara, A., Azuma, Y.T., Hata, F., et al. (2007) The active site cysteine of the proapoptotic protein glyceraldehyde-3-phosphate dehydrogenase is essential in oxidative stress-induced aggregation and cell death. *J. Biol. Chem.* 282: 26562–26574.

Negm, F.B. and Loescher, W.H. (1979) Detection and characterization of sorbitol dehydrogenase from apple callus tissue. *Plant Physiol.* 64: 69–73.

Negm, F.B. and Loescher, W.H. (1981) Characterization and partial purification of aldose-6-phosphate reductase (alditol-6-phosphate:NADP 1-oxidoreductase) from apple leaves. *Plant Physiol.* 67: 139–142.

Patel, S., Caplan, J. and Dinesh-Kumar, S. (2006) Autophagy in the control of programmed cell death. *Curr. Opin. Plant Biol.* 9: 391–396.

Pena, L.B., Pasquini, L.A., Tomaro, M.L. and Gallego, S.M. (2006) Proteolytic system in sunflower (*Helianthus annuus* L.) leaves under cadmium stress. *Plant Sci.* 171: 531–537.

Piattoni, C.V., Guerrero, S.A. and Iglesias, A.A. (2013) A differential redox regulation of the pathways metabolizing glyceraldehyde-3-phosphate tunes the production of reducing power in the cytosol of plant cells. *Int. J. Mol. Sci.* 14: 8073–8092.

Pommerrenig, B., Papini-Terzi, F.S. and Sauer, N. (2007) Differential regulation of sorbitol and sucrose loading into the phloem of *Plantago major* in response to salt stress. *Plant Physiol.* 144: 1029–1038.

Poole, L.B., Karplus, P.A. and Claiborne, A. (2004) Protein sulfenic acids in redox signaling. *Annu. Rev. Pharmacol. Toxicol.* 44: 325–347.

Ranney, T.G., Bassuk, N.L. and Whitlow, T.H. (1991) Osmotic adjustment and solute constituents in leaves and roots of water-stressed cherry (Prunus) trees. *J. Amer. Soc. Hortic. Sci.* 116: 684–688.

Rouhier, N., Gelhaye, E., Gualberto, J.M., Jordy, M.-N., De Fay, E., Hirasawa, M., et al. (2004) Poplar peroxiredoxin Q. A thioredoxin-linked chloroplast antioxidant functional in pathogen defense. *Plant Physiol.* 134: 1027–1038.

Rouhier, N., Lemaire, S.D. and Jacquot, J.-P. (2008) The role of glutathione in photosynthetic organisms: emerging functions for glutaredoxins and glutathionylation. *Annu. Rev. Plant Biol.* 59: 143–166.

Rumpho, M.E., Edwards, G.E. and Loescher, W.H. (1983) A pathway for photosynthetic carbon flow to mannitol in celery leaves: activity and localization of key enzymes. *Plant Physiol.* 73: 869–873.

Rychter, A.M., Rao, I.M. and Cardoso, J.A. (2016) Role of phosphorus in photosynthetic carbon assimilation and partitioning. In Handbook of Photosynthesis, 3rd edn. Eddited by Pessarakli, M. pp. 603–626. CRC Press, Boca Raton, FL.

Sakanishi, K., Kanayama, Y., Mori, H., Yamada, K. and Yamaki, S. (1998) Expression of the gene for NADP-dependent sorbitol-6-phosphate dehydrogenase in peach leaves of various developmental stages. *Plant Cell Physiol.* 39: 1372–1374.

Schafer, F.Q. and Buettner, G.R. (2001) Redox environment of the cell as viewed through the redox state of the glutathione disulfide/glutathione couple. *Free Radic. Biol. Med.* 30: 1191–1212.

Sengupta, D., Naik, D. and Reddy, A.R. (2015) Plant aldo-keto reductases (AKRs) as multi-tasking soldiers involved in diverse plant metabolic processes and stress defense: a structure–function update. *J. Plant Physiol.* 179: 40–55.

Shen, Y., Zhong, L., Markwell, S. and Cao, D. (2010) Thiol–disulfide exchanges modulate aldo-keto reductase family 1 member B10 activity and sensitivity to inhibitors. *Biochimie* 92: 530–537.

Stitt, M., Lunn, J. and Usadel, B. (2010) Arabidopsis and primary photosynthetic metabolism—more than the icing on the cake. *Plant J.* 61: 1067–1091.

Thompson, A.R. and Vierstra, R.D. (2005) Autophagic recycling: lessons from yeast help define the process in plants. *Curr. Opin. Plant Biol.* 8: 165–173.

Toroser, D., Athwal, G.S. and Huber, S.C. (1998) Site-specific regulatory interaction between spinach leaf sucrose-phosphate synthase and 14-3-3 proteins. *FEBS Lett.* 435: 110–114.

Vaitukaitis, J., Robbins, J.B., Nieschlag, E. and Ross, G.T. (1971) A method for producing specific antisera with small doses of immunogen. *J. Clin. Endocrinol. Metab.* 33: 988–991.

Velasco, R., Zharkikh, A., Affourtit, J., Dhingra, A., Cestaro, A., Kalyanaraman, A., et al. (2010) The genome of the domesticated apple (*Malus* × *domestica* Borkh.). *Nat. Genet.* 42: 833–839.

Verde, I., Abbott, A.G., Calabrin, S., Jung, S., Shu, S., Marroni, F., et al. (2013) The high-quality draft genome of peach (*Prunus persica*) identifies unique patterns of genetic diversity, domestication and genome evolution. *Nat. Genet.* 45: 487–494.

Williams, M.W. and Raese, J.T. (1974) Sorbitol in tracheal sap of apple as related to temperature. *Physiol. Plant.* 30: 49–52.

Xiong, Y., Contento, A.L., Nguyen, P.Q. and Bassham, D.C. (2007) Degradation of oxidized proteins by autophagy during oxidative stress in Arabidopsis. *Plant Physiol.* 143: 291–299.

Yadav, R. and Prasad, R. (2014) Identification and functional characterization of sorbitol-6-phosphate dehydrogenase protein from rice and structural elucidation by in silico approach. *Planta* 240: 223–238.

Yamaguchi, H., Kanayama, Y. and Yamaki, S. (1994) Purification and properties of NAD-dependent sorbitol dehydrogenase from apple fruit. *Plant Cell Physiol.* 35: 887–892.

Zhou, R., Cheng, L. and Wayne, R. (2003a) Purification and characterization of sorbitol-6-phosphate phosphatase from apple leaves. *Plant Sci.* 165: 227–232.

Zhou, R., Sicher, R.C., Cheng, L. and Quebedeaux, B. (2003b) Regulation of apple leaf aldose-6-phosphate reductase activity by inorganic phosphate and divalent cations. *Funct. Plant Biol.* 30: 1037–1043.